Available online at www.sciencedirect.com
ScienceDirect
Ultrasonics 48 (2008) 74–81
Ultrasonics
www.elsevier.com/locate/ultras

Capacitive micromachined ultrasonic transducers (CMUTs) with isolation posts

Yongli Huang [a], Xuefeng Zhuang [b,*], Edward O. Haeggstrom [c], A. Sanli Ergun [d], Ching-Hsiang Cheng [e], Butrus T. Khuri-Yakub [b]

[a] Kolo Technologies Inc., San Jose, CA, United States
[b] Edward L. Ginzton Laboratory, Stanford University, 450 Via Palou, Stanford, CA 94305, United States
[c] Electronics Research Unit, University of Helsinki, Helsinki, Finland
[d] Siemens Corporate Research, Mountain View, CA, United States
[e] Research Institute of Innovative Products and Technologies, The Hong Kong Polytechnic University, Hong Kong, China

Received 25 April 2007; received in revised form 12 November 2007; accepted 24 November 2007
Available online 14 December 2007

Abstract

In this paper, an improved design of a capacitive micromachined ultrasonic transducer (CMUT) is presented. The design improvement aims to address the reliability issues of a CMUT and to extend the device operation beyond the contact (collapse) voltage. The major design novelty is the isolation posts in the vacuum cavities of the CMUT cells instead of full-coverage insulation layers in conventional CMUTs. This eliminates the contact voltage drifting due to charging caused by the insulation layer, and enables repeatable CMUT operation in the post-contact regime. Ultrasonic tests of the CMUTs with isolation posts (PostCMUTs) in air (electrical input impedance and capacitance vs. bias voltage) and immersion (transmission and reception) indicate acoustic performance similar to that obtained from conventional CMUTs while no undesired side effects of this new design is observed.

Keywords: Ultrasound; Transducer; CMUT; Isolation posts; Charging; Hysteresis; Reliability

1. Introduction

Extensive research and development efforts to commercialize the CMUT as an alternative to piezoelectric ultrasonic transducers have been carried out during the last decade [1–8]. While CMUTs generally provide a wider bandwidth than current piezoelectric transducers [9], there are still issues to be addressed, such as device reliability [10] and performance improvement. For medical ultrasound applications, perhaps the most important concern is the need to increase the capability to image deep-laying structures in the human body [11] using CMUTs. Improved transduction efficiency boosting both output pressure and reception sensitivity is required. The output pressure is evaluated as the pressure generated per unit excitation voltage (kPa/VAC), whereas the reception sensitivity is judged by the detected voltage per unit impinging ultrasound pressure (mV/kPa). We introduce a CMUT featuring isolation posts (PostCMUT) as a solution to a device reliability problem during fabrication and operation. Furthermore, PostCMUTs can reliably operate beyond the contact voltage of the membranes to achieve improved transduction efficiencies.

Conventional CMUTs suffer from reliability issues because they feature a dielectric layer (silicon-nitride or silicon dioxide) in the vacuum cavities that trap electrical charges [16]. In the case of surface-micromachined CMUTs, the silicon-nitride dielectric layer is needed to selectively release the polysilicon sacrificial layer to form the cavities. In wafer-bonded CMUTs, the silicon dioxide

* Corresponding author.
E-mail address: xzhuang@stanford.edu (X. Zhuang).

0041-624X/$ - see front matter © 2007 Elsevier B.V. All rights reserved.
doi:10.1016/j.ultras.2007.11.006

layer in the cavity prevents electrical shorting between the conductive single crystal silicon membrane and the ground electrode underneath the cavity. Similar to the complementary metal-oxide-semiconductor (CMOS) devices in the integrated circuit industry, these dielectric layers in a CMUT can trap surface and interface charges [12,14,17,18]. Two major sources of trapped charges are the fabrication process and the strong electrical field within the transducer cavities during operation. The accumulation and distribution of the trapped charges depend on the specific fabrication run and the device operation history (e.g. DC bias, frequency and amplitude of the applied AC signal and duration of operation), causing unpredictable device contact voltage drift [15]. An additional problem is that the charges may create an electrostatic force that prevents the membrane from snapping back after contact [10]. It is worth noticing that the reliability issues of micro-electro-mechanical systems (MEMS) devices in general have been a hurdle towards commercialization [12–15]. For many other MEMS devices, electrical charges that reside in the dielectric layers of the MEMS devices are a major reliability concern.

For medical ultrasound, increased imaging depth can be achieved by improving the transduction efficiency of the transducers, accomplished by increasing the intensity of the electrical field in the CMUT vacuum cavities [19]. In conventional CMUTs operating in the pre-contact region, the contact voltage of the device limits the maximum efficiency. CMUTs operated in the post-contact region show higher transduction efficiency in transmission (TX) and sensitivity in reception (RX), than when they are operated in the pre-contact region. However, conventional CMUTs operated in the post-contact region suffer from hysteresis [16].

PostCMUTs perform comparably to conventional CMUTs in the pre-contact region [20]. Operation of PostCMUTs can be extended past the contact voltage into the post-contact region, allowing a higher output pressure, albeit not as high as in post-contact region operation [21] in conventional CMUTs. Most importantly, this gain in output pressure is possible without trapped charges in the devices or hysteresis in the device operation [16].

In [10], we presented capacitance–voltage (C–V) test results of PostCMUTs as a first validation of the charging-free operation of the PostCMUTs. In this paper, we present the design, fabrication, and acoustic characterization both in air (electrical input impedance) and in immersion (transmission, reception) of the PostCMUT device. All tests were performed in both conventional and post-contact modes. These test results are also compared to those from conventional CMUTs to show the improvements of the new design.

2. Design and fabrication

The basic structure of a CMUT is a parallel plate capacitor with a rigid bottom electrode, and a top electrode that resides on a flexible membrane Fig. 1a. The membrane transmits and detects acoustic waves in the adjacent medium [8]. To prevent electrical shorting of the devices, a conventional CMUT features at least one dielectric layer that fully covers one of its electrodes. In a PostCMUT, this protective layer is replaced by one or a few oxide posts protruding into the cavity from the bottom of the cavity. The oxide isolation posts that substitute for a dielectric isolation layer between their electrodes are of desired height, size and location. Fig. 1b shows the schematic cross-sectional view of a PostCMUT.

There are three major design criteria for PostCMUTs: (1) the area of the oxide posts should be small enough that charges trapped in them have a negligible effect on device operation while still be compatible with the buffered oxide etching (BOE) fabrication process that forms the posts; (2) the post configuration should prevent the devices from shorting in the entire region of operation; and (3) if post-contact operation is required, the configuration of the posts should provide, without hysteresis, the frequency response desired after the membrane makes contact with the posts.

Because the bottom surfaces of their cavities are patterned, PostCMUTs are difficult to manufacture by surface-micromachining. The reason is that for the surface-micromachining process, the polysilicon sacrificial layer covers the isolation posts in a conformal fashion. In this study, the PostCMUTs were fabricated by a wafer-bonding technique [8], with one additional lithography and BOE step: patterning of the silicon oxide layer using a post-feature mask. This step was performed before the wafer-bonding step. The major steps of the fabrication process flow are shown in Fig. 2. The added step is straightforward and did not affect device yield. Fig. 3 shows photographs of PostCMUTs with various post patterns. The point dimension and line width in the post pattern were 3 μm by 3 μm, and 3 μm, respectively. The PostCMUTs were fabricated with square, single crystal silicon membranes that were 1 μm thick, with a side length of either 88 μm or 102 μm. The oxide post height was 0.3 μm, in a 1 μm deep cavity.

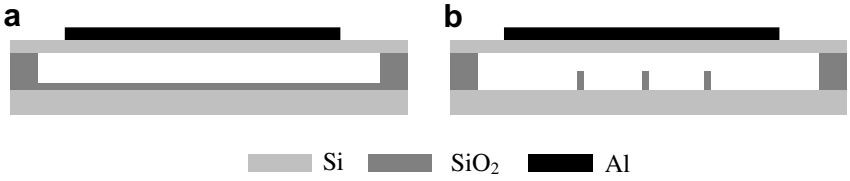

Fig. 1. Schematic cross-section of (a) conventional CMUT and (b) PostCMUT.

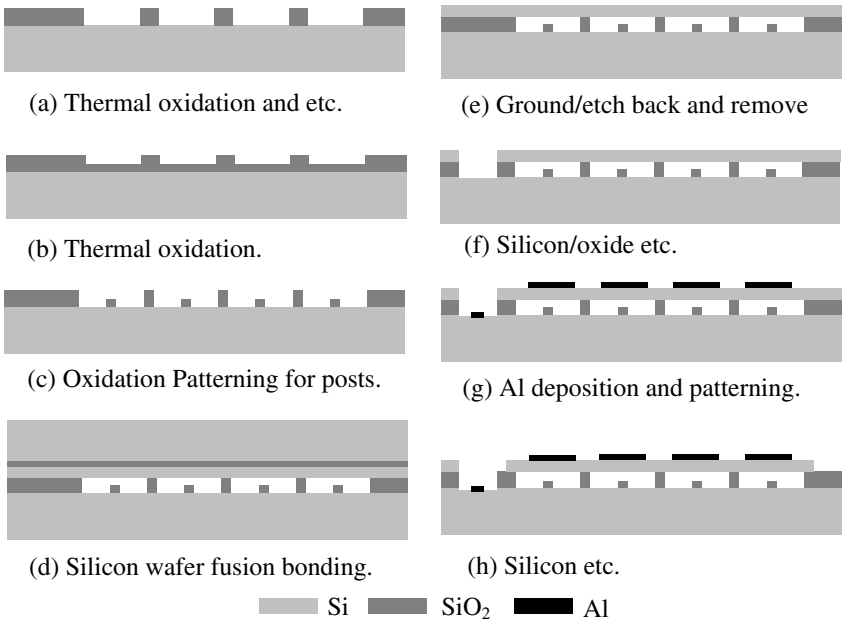

Fig. 2. Major steps of PostCMUT fabrication process.

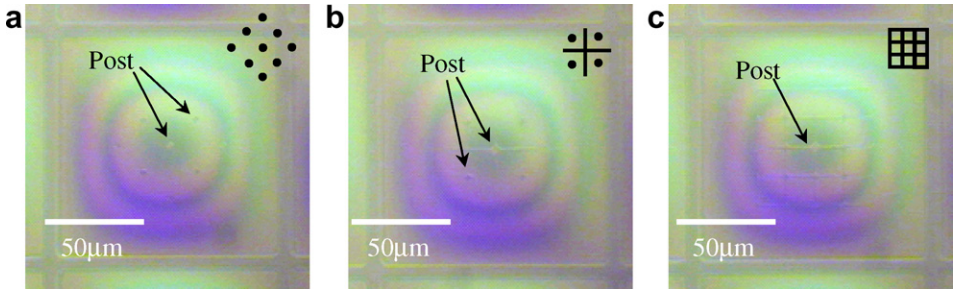

Fig. 3. Photographs of fabricated devices with different post patterns showed in the top right corners: (a) 9-point pattern (b) cross pattern and (c) net pattern.

Table 1
Summary of device parameters

Device	Conventional CMUT		PostCMUT	
	A	B	C	D
Membrane thickness (μm)	1	1	1	1
Membrane width (μm)	88	102	88	102
Total device dimension (μm^2)	550 × 6000	550 × 6000	550 × 6000	550 × 6000
Electrode separation (μm)	1	1	1	1
Insulation layer/post thickness (μm)	0.3	0.3	0.3	0.3
Contact voltage (V)	~60	~40	~40	~82

Conventional CMUTs with identical membrane and cavity dimensions (but with a fully covered 0.3 μm thick oxide layer) were fabricated for comparison. For example, the total transverse oxide post area of a 9-point PostCMUT was 81 μm^2, which is 1.05% of the oxide area of the conventional CMUTs carrying membranes with 88 μm side length. The element size, approximately 0.55 mm by 6 mm, was almost the same in all the devices. Device parameters are summarized in Table 1.

3. Device characterization

The PostCMUT characterization included measurements of electrical input impedance in air, C–V measurements, and TX and RX measurements in immersion. All tests were performed in both pre-contact and post-contact modes.

In the electrical input impedance measurements in air, a network analyzer (Model 8751, Hewlett-Packard Company, Palo Alto, CA) and a DC voltage supply (Model PS310, Stanford Research Systems, Sunnyvale, CA) were used to measure electrical input impedance of the CMUTs at different DC bias conditions.

In the C–V measurements, a DC source applied a negative DC bias on the CMUT, and a signal generator generated a 5 kHz, 60 mVp-p, AC signal. An oscilloscope was

used to measure the signal from a voltage divider that consists of a 130 kΩ resistor and the CMUT carrying membranes with 88 μm side length.

In the TX measurements in immersion, the distance between the hydrophone and the CMUT transmitter was 11 mm (Seki = 1.05[1]). First, conventional CMUTs carrying membranes with 88 μm side length were compared to PostCMUTs carrying membranes with 102 μm side length because they have almost the same contact voltage of approximately 45 V. The comparison focused on their relative TX transduction efficiency. In this test, a 2.5 MHz sinusoidal wave train with 30 cycles and an amplitude of 5 V was applied to the CMUT. A receiving hydrophone (PZT-Z44-0400, Specialty Engineering Associates) was positioned by an Aerotech HDZ2 linear translation stage with an accuracy of 1 μm. Before it was read into the oscilloscope, the signal from the hydrophone was amplified by a 20 dB, 0.1 MHz to 400 MHz bandwidth, 50 Ω preamplifier (HP 8447 A). The transducers were aligned for maximum reception voltage. Second, conventional CMUTs carrying membranes with 88 μm side length were compared to PostCMUTs carrying membranes with 88 μm side length for output spectra. In these tests, a +5 V step signal with a 6 ns rise time was applied to the CMUTs.

In the RX measurements, the distance between the PZT transducer and the CMUT was 86.1 mm (Seki = 1.1). First, the same 88 μm conventional CMUTs were compared to the 102 μm PostCMUTs used in the initial TX tests for reception sensitivity. A 2.5 MHz, 5 Vp-p sinusoidal, 35–50 cycle wave train was applied to the transmitting 12.5 mm diameter circular flat focus piezoelectric transducer (Panametrics V109). The amplitude of the received signal was measured as a function of the bias voltage applied to the CMUT, and as a function of AC amplitude applied to the transmitting V109 transducer. Second, the same 88 μm conventional CMUTs were compared to the 88 μm PostCMUTs that had been assessed in the initial TX tests for output spectra. The +5 V step signal was applied to the Panametrics transducer. A reception calibration experiment was carried out to calculate the sensitivity of the CMUT, in which the CMUT was exchanged for the hydrophone to determine the acoustic pressure generated by the piezoelectric transducer onto the CMUT surface.

4. Results and discussion

The electrical input impedance of both the conventional CMUTs and the PostCMUTs obtained in air is shown in Fig. 4. Before contact, the impedance curves of three different PostCMUTs were nearly identical. After contact, the locations of the resonance peaks in the impedance curves were slightly different. Because the device resonances in air are determined by the membrane resonance and the electrostatic spring softening [23], these results were expected. Since all CMUTs in this measurement carried membranes of the same dimensions, and since the spring softening effect is small at low bias voltages, the resonance peaks of the different devices appeared at almost the same frequency in the impedance curves at low bias voltages, i.e., before membrane–cavity contact. After contact, the device membranes were anchored at their center; hence, the membrane size was no longer defined by the perimeter of the square membranes. After contact, the central contact area of the conventional CMUT is larger than that of the PostCMUT, resulting in a smaller equivalent membrane size (the size of the membrane that is free to move) for the conventional CMUT than for the PostCMUT. Therefore, after contact, the resonance frequency of the conventional CMUT is higher than that of the PostCMUT. Furthermore, the contact area of the conventional CMUT after contact increases with bias voltage. Hence the equivalent membrane size of the conventional CMUT after contact decreases with increasing bias voltage. In contrast to this, the contact area of the PostCMUT is constant and is determined by the top surface of the posts only. This is important because after contact, the equivalent membrane size of the PostCMUT is independent of the bias voltage. Therefore, unlike the conventional CMUT, the PostCMUT exhibits a frequency response that is largely independent of bias voltage after contact Fig. 4d.

A brief comparison of the capacitance–voltage (C–V) test results between PostCMUTs and conventional CMUTs has been reported in [10] as a first validation of the charging-free operation of PostCMUTs. In all of our tests, charging was always observed in conventional CMUTs, and never observed in PostCMUTs.

No hysteresis was observed after the membrane had been in contact with the posts, either in the ultrasonic transmission tests, Fig. 6b, or in the reception tests, Fig. 5b. Thus, as expected from the C–V tests, the PostCMUT design remedied the hysteresis seen with conventional CMUTs operating in the post-contact region [10].

It is evident in Figs. 5 and 6 that the PostCMUT and the conventional CMUT show comparable performance before membrane-post-contact. After contact, the PostCMUT allowed application of a higher bias voltage, and hence, gained a corresponding performance increase without suffering from hysteresis or charging. Compared to conventional CMUTs operated in post-contact region, the PostCMUTs showed less transmission and reception efficiency, but also exhibited negligible hysteresis and charging. We measured, after contact, 6.25 kPa/VAC transmission efficiency and 8.25 mV/kPa reception sensitivity. Both measurements were made at 70 VDC, with a

[1] The Seki parameter describing diffraction effects in the acoustic field emitted by a piston transducer [22] is an approximate way to tell whether the measurements are performed in the near field or in the far field. "Seki = 1.05" tells that the measurements were performed in the far field. The parameter is defined as $S = (d^* \lambda)/a^2$, where d is the distance from the transducer surface along the acoustic axis, λ is the sound wave length in the immersion medium, and a is the dominant length scale of the transducer (radius or 0.5*max side length of a rectangular transducer).

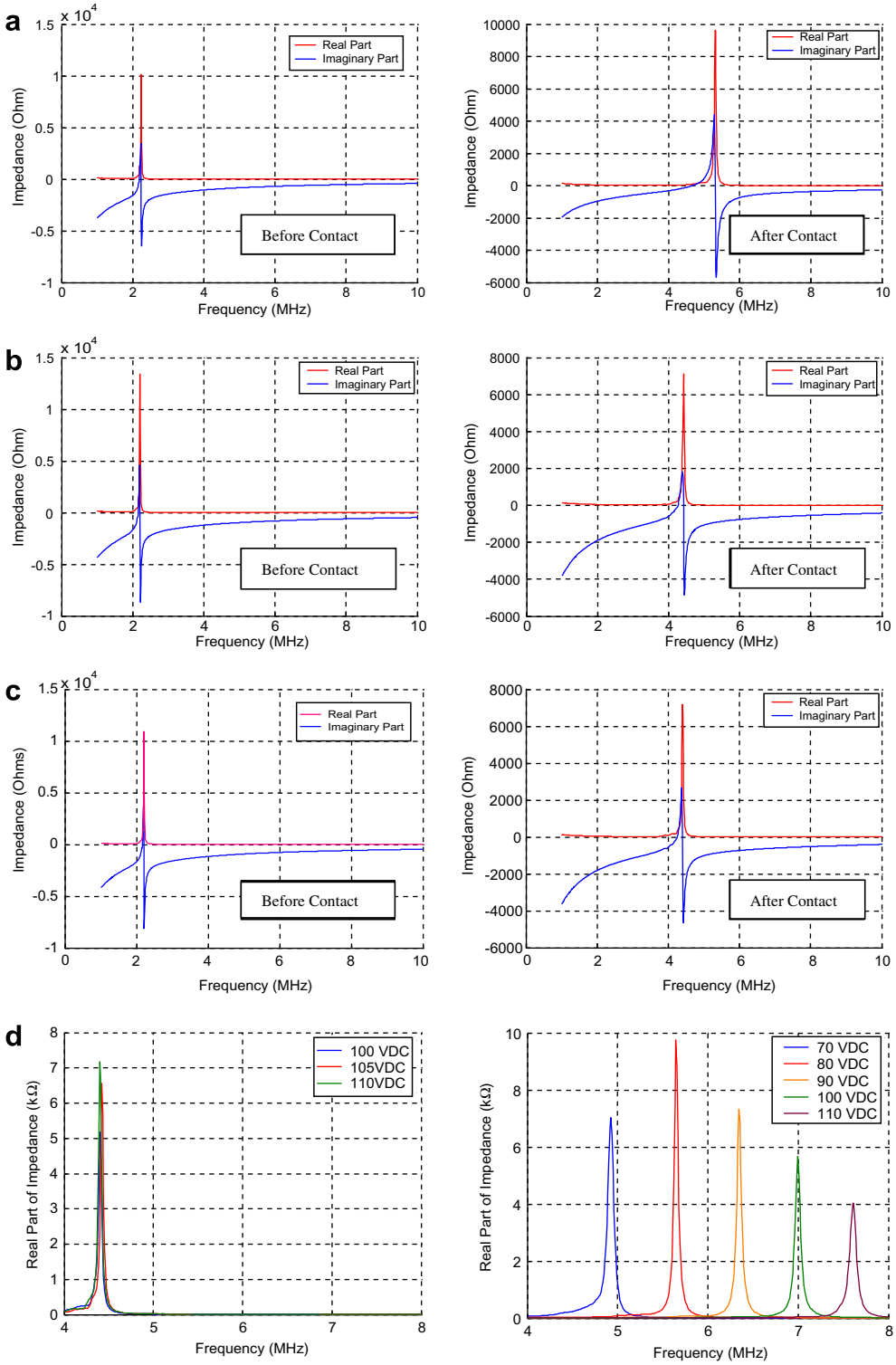

Fig. 4. Electrical input impedance of (a) conventional CMUT, (b) PostCMUT with 5-point post pattern and (c) PostCMUT with cross post pattern. For PostCMUT, the impedance was measured at 70 V and 110 V bias voltage, before and after contact, respectively. For conventional CMUTs, the impedance was measured at 40 V and 80 V bias voltage, before and after contact, respectively. (d) (left) the real part of impedance of a postCMUT with cross post pattern at different bias voltage after contact (right) the real part of impedance of a conventional CMUT at different bias voltages after contact.

2.5 MHz signal. The uncorrected fractional bandwidth in transmission was 163%, with the same bias voltage. The corresponding numbers for the conventional CMUTs were 16 kPa/VAC, 25 mV/kPa, and 149%, respectively. In pre-contact (35 VDC), the corresponding numbers were 2.75 kPa/VAC for transmission efficiency, 3.75 mV/kPa for reception sensitivity, and 123% for uncorrected fractional bandwidth. The corresponding numbers for the con-

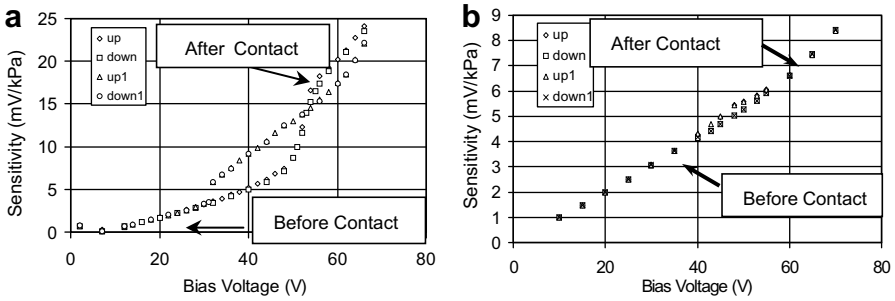

Fig. 5. Ultrasonic reception by CMUT as a function of bias voltage. Source: a PZT transducer with a constant output. (a) Conventional CMUT: hysteresis is evident after membrane-bottom electrode contact (collapsed region operation). (b) PostCMUT: good repeatability.

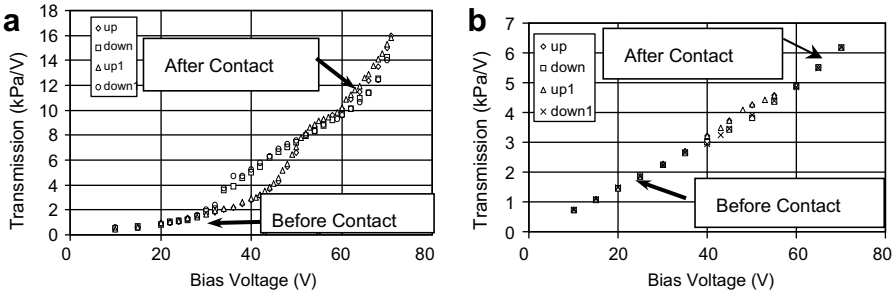

Fig. 6. Ultrasonic transmission by CMUT received by a broad band hydrophone as a function of bias voltage. (a) Conventional CMUT: hysteresis is evident after membrane-bottom electrode contact (collapsed region operation). (b) PostCMUT: good repeatability.

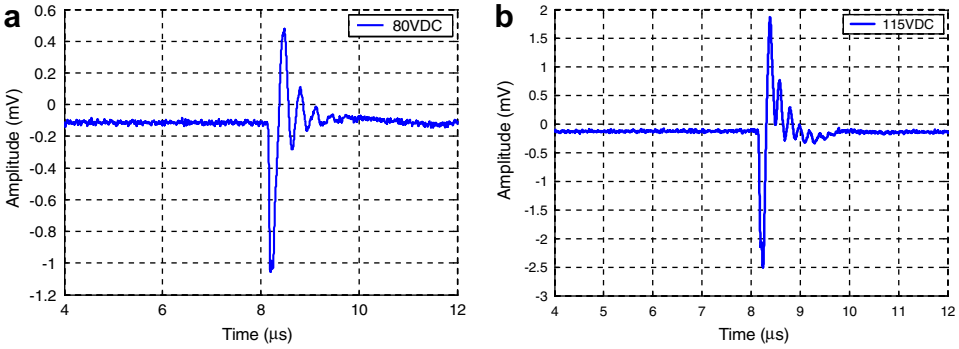

Fig. 7. Transmission pulses obtained by a hydrophone from a PostCMUT operating (a) before contact and (b) after contact. The input AC signal was a 5 V step function. Bias voltages are 80 V and 115 V for the measurements before contact and after contact, respectively.

ventional CMUTs were 2.1 kPa/VAC, 4.1 mV/kPa, and 136%.

Waveforms transmitted by PostCMUTs and conventional CMUTs and their spectra are shown in Figs. 7–10. Before contact, the spectra of both PostCMUTs and conventional CMUTs look similar. After contact, the high frequency cut-off of the PostCMUTs did not change as a function of bias voltage because its membrane shape did not change with increasing bias voltage. For conventional CMUTs, however, increasing the bias voltage after contact adds contact area between the membrane and the cavity floor. Consequently, the size of the membrane that is free to move decreases. Thus the membrane of the CMUT becomes relatively stiff and the resonant frequency of the CMUT increases. This increases the higher cut-off frequency.

5. Conclusions

The results indicate that incorporating isolation posts into the CMUT design remedies the device reliability problem caused by charging. The PostCMUTs eliminate post-contact mode operation hysteresis seen in conventional CMUTs and therefore enables reliable CMUT operation in the post-contact region. No deleterious side effects of the new design were observed in the ultrasonic tests. The PostCMUTs were fabricated using a slight modification of a newly developed process (based on the wafer-bonding

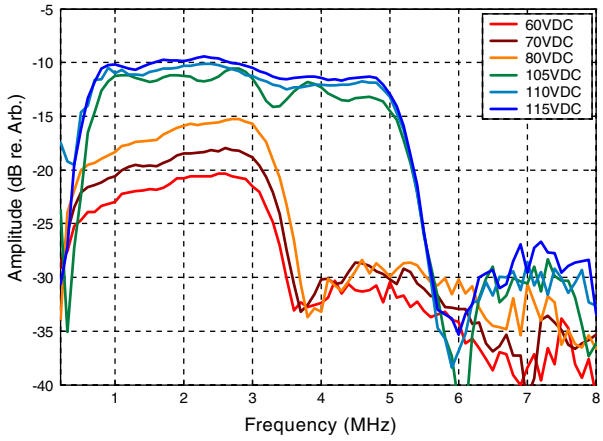

Fig. 8. Transmission spectrum (not corrected for medium attenuation or diffraction) of a PostCMUT at different bias voltages. The device operated in pre-contact region when the bias voltage is smaller than 80 V and in post-contact region when the bias voltage is larger than 105 V.

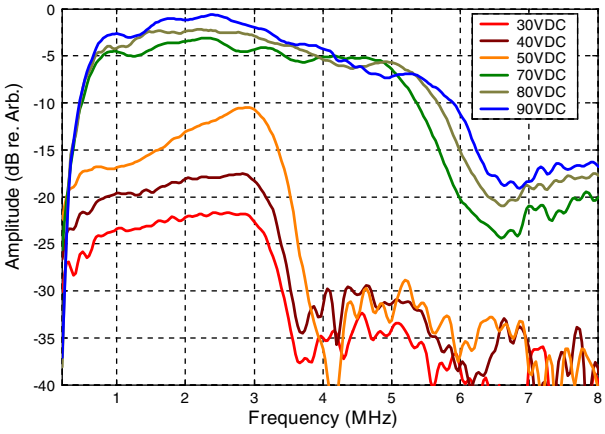

Fig. 10. Transmission spectrum (not corrected for medium attenuation or diffraction) of a Conventional CMUT at different bias voltages. The device operated in pre-contact region when the bias voltage is smaller than 50 V and in post-contact region when the bias voltage is larger than 70 V.

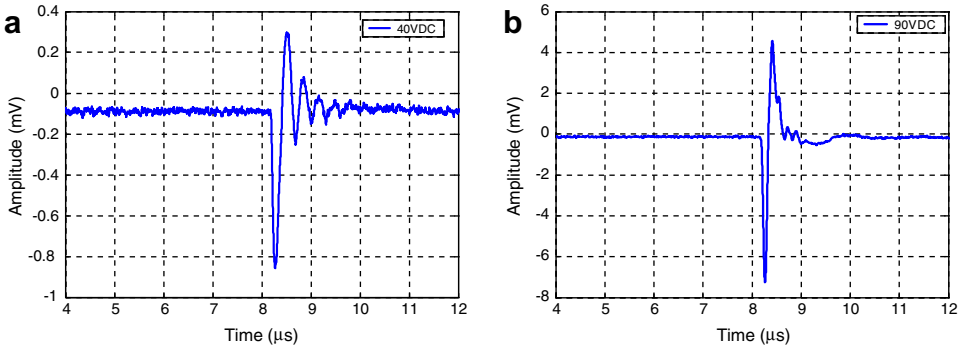

Fig. 9. Transmission pulses obtained by a hydrophone from a Conventional CMUT operating (a) before contact and (b) after contact. The input AC signal was a 5 V step function. Bias voltages are 40 V and 90 V for the measurements before contact and after contact, respectively.

technique) that has improved the reliability of the CMUTs. The process modification to the process flow is straightforward and does not impact the device yield.

The experimental results obtained with the PostCMUTs operating in the post-contact region showed that these devices reveal gains in maximum output pressure and reception sensitivity, compared to CMUTs operating in the conventional region. In addition, the fractional bandwidth of the PostCMUT was larger than the fractional bandwidth of CMUTs operated in the conventional region.

Acknowledgements

The authors would like to acknowledge the financial support of ONR and NIH. We would also like to thank Dr. Utkan Demirci, Dr. G. Göksenin Yaralioglu and the staff in Edward L. Ginzton Laboratory at Stanford University for their assistance. Xuefeng Zhuang was supported by a Weiland Family Stanford Graduate Fellowship. Dr. Hæggström acknowledges the Wihuri-Foundation and the Academy of Finland for financial support. Work was performed in part at the Stanford Nanofabrication Facility of NNIN supported by the National Science Foundation under Grant ECS-9731293.

References

[1] X.C. Jin et al., Fabrication and characterization of surface-micromachined capacitive ultrasonic transducers, J. Microelectromech. Syst. 8 (1999) 100–114.
[2] D. Hohm, G. Hess, A subminiature condenser microphone with silicon-nitride membrane and silicon backplate, J. Acoust. Soc. Am. 85 (1) (1989) 476–480.
[3] D.W. Schindel et al., The design and characterization of micromachined air-coupled capacitance transducers, IEEE Transactions on UFFC 42 (1) (1995) 42–50.
[4] M. Rafiq, C. Wykes, The performance of capacitive ultrasonic transducers using v-grooved backplates, Meas. Sci. Technol. 2 (2) (1991) 168–174.
[5] E. Cianci et al., Fabrication of capacitive ultrasonic transducers by a low temperature and fully surface-micromachined process, Precis. Eng. 26 (4) (2002) 347–354.
[6] A. Caronti et al., The effects of membrane metallization in capacitive microfabricated ultrasonic transducers, J. Acoust. Soc. Am. 115 (2) (2004) 651–657.
[7] P. Eccardt et al., Micromachined transducers in CMOS technology, Proceedings of Ultrasonics Symposium (1996) 959–962.

[8] Y. Huang et al., Fabricating capacitive micromachined ultrasonic transducers with wafer-bonding technology, J. Microelectromech. Syst. 12 (2003) 128–137.
[9] J.F. Gelly et al., Comparison of piezoelectric (thickness mode) and MEMS transducers, in: Proceedings of 2003 IEEE Ultrasonics Symposium, Hawaii, October 6–9, 2003.
[10] Y. Huang et al., A solution to the charging problems in capacitive micromachined ultrasonic transducers (CMUTs), IEEE Transactions on UFFC 52 (4) (2005) 578–580.
[11] D.M. Mills, Medical imaging with capacitive micromachined ultrasound transducer (CMUT) arrays, in: Proceedings of 2004 IEEE Ultrasonics Symposium, Montréal, August 24–27, 2004.
[12] C. Goldsmith, Lifetime characterization of capacitive RF MEMS switches, in: Microwave Symposium digest 2001, IEEE MTT-S International, vol. 1, May 20–25, 2001, pp. 227–230.
[13] J. DeNatale et al., RF MEMS reliability, in: The 12th International Conference on Solid State Sensors, Actuators and Microsystems, Boston, June 8–12, 2003, pp. 943–946.
[14] J.R. Reid, Capacitive switch reliability issues, in: Proceedings of the Government Microcircuit Application Conference (GOMAC), March 2002, pp. 48–51.
[15] M.W. Kowarz et al., Method and System for Actuating Electro-Mechanical Ribbon Elements in Accordance to a Data Stream, US Patent 6,144,481, November 7, 2000.
[16] Y. Huang et al., Comparison of conventional and collapsed region operation of capacitive micromachined ultrasonic transducers, IEEE Transactions on UFFC 53 (10) (2006) 1918–1933.
[17] J.R. Reid, Dielectric charging effects on capacitive MEMS actuators, in: IEEE MTT-S International Microwave Symposium, RF MEMS Workshop, Phoenix, AZ, May 2001.
[18] H. Amjadi et al., Charge storage in double layers of silicon dioxide and silicon nitride, in: 9th International Symposium on Electrets, September 25–30, 1996, pp. 22–27.
[19] I. Ladabaum et al., Surface-micromachined capacitive ultrasonic transducers, IEEE Transactions on UFFC 45 (May) (1998) 678–690.
[20] Y. Huang et al., Capacitive micromachined ultrasonic transducers (cMUTs) with isolation posts, Presented at the 2004 IEEE International Ultrasonics Symposium, Montréal, QC, Canada, August 23–27, 2004.
[21] B. Bayram et al., A new regime for operating capacitive micromachined ultrasonic transducers, IEEE Transactions on UFFC 50 (9) (2003) 1184–1190.
[22] H. Seki et al., Diffraction effects in the ultrasonic field of a piston source and their importance in accurate measurement of attenuation, J. Acoust. Soc. Am. 28 (2) (1956).
[23] V.L. Rabinovitch et al., Prediction of mode frequency shifts due to electrostatic bias, in: Technical Proceedings of the 10th International Conference on Solid-State Sensors and Actuators, Transducers, June 7–10, 1999, Sendai, Japan.